Dissociation kinetics at polyacrylic latex-coated electrodes

Tianbao Li, Koichi Aoki*, Jingyuan Chen, Toyohiko Nishiumi

Department of Applied Physics, University of Fukui, 3-9-1, Bunkyo, Fukui-shi, 910-8507 Japan

Abstract

Polystyrene/poly(acrylic acid) latex particles 0.26 μm in diameter, which were synthesized by emulsion copolymerization of styrene and acrylic acid, were immobilized on the platinum electrode in a uniform film. The film did not block the diffusion current of a ferrocene derivative in the solution. The voltammograms showed the reduction of hydrogen ion, which was supplied not only from the solution but also from the dissociation of carboxyl acid of the adsorbed latex. The peak currents at pH less than 4.5 were proportional to the thickness of the latex film, and were supplied by dissociation from the latex. In contrast, those at pH more than 5.5 were independent of the film thickness, and were controlled by the dissociation kinetics of the carboxyl acid within the first particle layer. Expressions for the voltammetric currents with the CE mechanism were derived theoretically. The theory predicts that the reaction rate constant can be evaluated from the lower deviation from the proportionality of the peak currents to scan rates, as in consistent with the experimental results. The rate constant was by one order smaller than the homogeneous rate constant of acrylic acid. pH-Titration demonstrated the electrostatic interaction of $-COO^-$, like in self-assembled carboxylate films. The average concentration of carboxylate in the latex was ca 2.7 M. The dissociation was limited to the surface domain of the latex.

key words: polyacrylic latex-coated electrodes; voltammetric CE mechanism; electrostatic interaction; theoretical analysis

* Corresponding author: e-mail kaoki@u-fukui.ac.jp, phone +81 776 27 8665

1. Introduction

Poly(acrylic acid) (PAA) has been used electrochemically for uptake of redox cations, e.g., bis-bipyridyl cobalt [1,2], cadmium in the presence of alumina [3], cupper [4], tris(2,2'-bipyridyl)ruthenium [5], nickel(II) tetraazamacrocyclic complex [6], bis-bipyridyl osmium [7], hexaammineruthenium and hexaamminecobalt [8], ferrocenylethanol [9], thallium [10], some alkali metal hydroxides without salts [11], and *N,N*-dimethylaminomethyl-ferrocene [12]. Negatively charged molecules such as hexacyanoferrate cannot be simply taken up to PAA [5]. PAA can immobilize cytochrome c [13] and big particles such as multiwalled carbon nanotubes [14], gold nanoparticles [15], CdS nanoparticles with cupper ion [16], and platinum nanocrystals [17]. It makes copolymers with polyaniline [18,19] and has immobilized flavin adenin dinucleotide for detection of glucose [20].

The uptake of cations to PAA is caused by association of the carboxyl moiety in PAA, and hence a degree of the uptake should be determined by the pK_a as well as pH in solution [5,9], as is predicted from the association in acetic acid. When PAA is in a solid state or a film, the association is complicated by block of a loss of permeation of solvent and ions. It is also hindered by electrostatic interaction of the deprotonated carboxyl group [9], as has been found in carboxyl alkanethiol self-assembled monolayers [21-23]. In order to control quantitatively a degree of the association, PAA has to be dispersed in solution [10,11], or such PAA films have been employed that all the acrylic moiety might be exposed to solution [20,24]. Another technique of enhancing the ion-exchange ability of PAA is to make polymers be microparticles, that is, latex particles. Latex suspensions of PAA have been used for the uptake of trimethylaminoferrocene, depending on pH and salt concentrations [25].

Functionalized redox latexes are useful for enhancement of electrochemical responses either in film forms or in suspensions. Hemin-immobilized polyallylamine-polystyrene latex has increased catalytic efficiency of reduction of dioxygen [26] and

carbon dioxide [27]. The latex composed of polystyrene sulfonate, polyallylamine and tyrosinase showed catalytic currents for the enzymatic oxidation of catechol to o-quinone [28]. Gold particles-included latex with DNA probes has enabled to detect 0.5 fM DNA hybridization [15]. Advantages of these applications are ascribed not only to efficient immobilization of catalysis but also to fast mass transport of large surface area of particles owing to high porosity, permeability and swollenness. However, the redox reaction is sometimes blocked by a loss of freedom the redox sites on the latex. For example, ferrocenyl latexes have been partially oxidized at electrodes by geometrical restriction of reaction zone [29-32] or rotational diffusion [33,34]. Geometrical hindrance of the polyaniline latex has given rise to unpredicted behavior such as oscillation currents [35], discrete currents independent of the latex concentration [36], and the irreversible waves due to the electric percolation [37].

Since PAA can immobilize various cations in aqueous solutions, its latex has potential applications to electrochemical control of ion exchange. Unfortunately, few data on physicochemical properties of PAA latex have been reported as for the dissociation equilibrium, dissociation kinetics and blocking of mass transport [15,25], to our knowledge. In order to build up PAA latexes in synthesis, it is important to get a value of pK_a, pH dependence in the dissociation of the carboxyl group, permeability of ions and solvents into the latex, thickness of the chemical and electrochemical reaction zones within the latex, and the dissociation rate constant. This research was triggered to shed light on these properties, and is devoted to investigating especially the electrochemical reduction of hydrogen ion dissociated from the adsorbed PAA latex.

2. Experimental

2.1 Chemicals

The polystyrene/poly(acrylic acid) (denoted as PAAPS) latex was synthesized by

copolymerization of styrene and acrylic acid at the loaded molar ratio, 1.0 : 0.076, in emulsions with the help of sodium dodecylsulfate (SDS), as has been described [25]. (Ferrocenylmethyl)trimethyl- ammonium bromide (FcTMA) was synthesized according to the bibliography [38], and was purified by re-crystallization. Other chemicals were of analytical grade, and were used as received. Aqueous solutions were prepared with ion-exchanged deionized water of which resistivity was ca. 12 MΩ cm.

2.2. Measurements and instrumentation

Cyclic voltammetry was carried out with a computer-controlled potentiostat, Compactstat (Ivium Tech., Netherlands). The working electrode was a platinum disk 0.8 mm in radius. The reference electrode was an Ag|AgCl (3.0 M NaCl), and the counter electrode was a platinum coil. The surface of the working electrode was polished with 0.03 μm alumina paste on a wet cotton, and was rinsed with distilled water in an ultrasonic bath three times before each voltammetric run.

The size of the latex particles was determined by a scanning electron microscope (SEM, Hitachi, S-2600H). The size distribution and particle-dispersion were determined by a light scattering instrument (Malvern Zetasizer Nano-ZS). A conductometer was HEC-110 (DKK, Tokyo). The UV-spectrometer was V-570 (JASCO, Tokyo).

3. Results

3.1 Ionic properties of PAAPS suspensions

The PAAPS latex particles were spherical $2r = 0.265 \pm 0.011$ μm in diameter by SEM photographs, where the error means the standard deviation obtained from randomly selected 50 particles. The diameter was consistent with the value obtained from the dynamic light scattering. The suspension in a glass vessel exhibited iridescence

on the wall of the vessel [25], and must form a colloidal crystal near the wall. The dried suspension on a glass plate formed a two-dimensional hexagonal arrangement, according to SEM observation [25].

The suspension was ion-exchanged to acidic form by addition of 0.1 M HCl and then was deionized iteratively by centrifugation and re-dispersion with deionized water. An aliquot of the suspension was titrated with NaOH solution on monitoring the electric conduction. The conductance at the beginning of the titration did not vary with the addition of NaOH, and then increased rapidly with the added volume. The dissociation seems to proceed in

$$\text{(latex)-COOH} + \text{OH}^- \rightarrow \text{(latex)-COO}^- + \text{H}_2\text{O}$$

From the amount of NaOH at the end point of the titration (x mol), the dried amount of the aliquot (w g) and the density of the latex (d = 1.05 g cm^{-3}), the number of carboxyl group per particle was $xN_A(d\ 4\pi r^3/3)/w = 5.32\times10^5$, where N_A is the Avogadro constant. Since the value of x did not vary with the titration time or stirring speed of the solution, it should be close to the equilibrium value.

It is not certain, however, whether the dissociation occurred on the surface of the latex or within the latex. We dissolved given weights of the latex, polystyrene (PS) and PAA sufficiently in dichloromethane and obtained their UV spectra. The spectra had a band at ca. 260 nm, being not specific to PS or PAA. The absorbances, A, of both PS and PAA at 260 nm were proportional to their concentrations, c_s and c_s, respectively, that is, $A_s = \varepsilon_s c_s$ and $A_a = \varepsilon_a c_a$ with $\varepsilon_a/\varepsilon_s = 3.59$. Since the latex is composed of PS and PAA, the absorbance should be expressed by $A = A_s + A_a = \varepsilon_s c_s + \varepsilon_a c_a$. In contrast, the concentration of the latex is given by $c = c_s + c_a$. From known values of ε_s, ε_a, c and A, we evaluated c_s and c_a, yielding the number of carboxyl group per particle to be 1.58×10^7. This value corresponds to 2.7 M in concentration if the carboxylic group is uniformly distributed in one particle. The much smaller value of the amount by the conductometric titration than this value indicates that the carboxylic acid only on the surface should participate in the dissociation. Letting the thickness of the surface active

domain be δ, the algebra $(4\pi r^2\delta)/(4\pi r^3/3) = 5.32/158$ yields $\delta = 1.5$ nm at $r = 0.265/2$ μm. Thus the dissociation is limited only to a domain of a few molecular layers of the latex.

The molar ratio of PAA to PS per particle was $c_a/c_s = 0.34$ by the absorbance. The inequality, $c_a < c_s$, suggests hydrophobicity of the latex owing to PS. This is a reason why the dissociation was restricted only to the surface domain of the latex. The ratio was five times as large as the ratio (0.076) of the loaded amount in the synthesis, indicating more favorable polymerization of PAA than PS in the emulsion.

In order to evaluate acidic properties of the PAAPS latex, the suspension was titrated with NaOH solution on monitoring pH of the solution. The suspension before the titration was taken to be acidic form by being stirred in 0.1 M HCl solution for two days, and being centrifuged with ultrapure water three times. Although a stoichiometric point could be identified from the titration curve, as is shown in Fig. 1, the titration curve was deviated from a typical sigmoid especially for pH less than 7.0. In order to quantify the deviation, we re-plotted the pH-variation with $\log(x/(1-x))$ in Fig. 2, where x is the ratio of the titrated volume of NaOH to that at the end point. The plot fell on a line ((a) in Fig. 2). The titration curve of a weak acid is approximately expressed by

$$\mathrm{pH} = \log[x/(1 - x)] + \mathrm{p}K_a \qquad (1)$$

Here $\mathrm{p}K_a$ can be evaluated from a line with unity slope at $x = 0.5$. The plot in Fig. 2 provides $\mathrm{p}K_a = 5.3$ at $x = 0.5$. The slope of the line was 2.0, whereas that in Eq. (1) is unity. The larger value of the slope than unity can be ascribed to (i) wide distribution of $\mathrm{p}K_a$ caused by distribution of molecular weight of the polymers and (ii) electrostatic interaction of carboxylate owing to its high concentration in the latex. Reason (i) is intrinsic to configuration of the polymer, while (ii) depends on concentration. We diluted the PAAPS latex in mixture of THF and water, and titrated it with NaOH solution. The logarithmic titration curve (b) obeyed Eq. (1) for $\log[x/(1-x)] < 0.2$, as is shown in Fig. 2. Therefore, the larger slope in Fig. 2(a) is not ascribed to a distribution of various values of $\mathrm{p}K_a$, but must be caused by such high density of deprotonated

carboxyl acid that the electrostatic repulsion among -COO^- may hinder the dissociation. The electrostatic repulsion has been demonstrated [21] for the self-assembled film of ω-carboxylalkanethiol in (c) of Fig.2. Since the latex contains concentration of carboxylate as high as 2.7 M, electrostatic repulsion is necessarily conspicurous at the cost of electric neutrality by salt in solution.

3.2. Voltammetric features of PAAPS latex at low pH

Voltammetry was performed in aqueous solution including FcTMA at various pH values adjusted with HCl. FcTMA was added deliberately to the solution not only because of avoiding incorrect potential by accidental coating the reference electrode with the latex film but also because of evaluating a blocking of mass transport by the adsorbed latex. Voltammograms of the solution including 0.23 mM HCl + 0.20 mM FcTMA + 0.5 M KCl showed well-defined redox peaks at ca. -0.5 V and 0.4 V, as are shown in Fig. 3(a). Since the cathodic peak current at -0.5 V was proportional to concentrations of H^+, it can be attributed to the reduction of H^+. The anodic current at 0.4 V is ascribed to the oxidation of FcTMA. These peak currents were proportional to the square-root of the potential scan rate, v. Therefore they are controlled by diffusion of H^+ or FcTMA from the bulk. The diffusion coefficients were evaluated from the slopes to be $D_H = 5.4\times10^{-5}$ cm^2 s^{-1} and $D_{FcTMA} = 0.56\times10^{-5}$ cm^2 s^{-1}. PAA is adsorbed strongly on electrodes at low pH values reportedly [39], because PAA is associated with H^+ to take an electrically neutralized form. In fact, a deposit was viewed on the electrode surface after the voltammetry. Nevertheless, the diffusion current was not blocked, suggesting good ion-permeability into the latex particle and vacancy among adsorbed latex spheres.

The non-blocking property inspired us to coat the electrode deliberately with the PAAPS latex by casting a given amount of latex suspension and being dried. We designate it as the H_2O-PAAPS-coated electrode The voltammogram in the same

solution as above showed the cathodic current of H^+ larger than that at the bare electrode (in Fig 3(b)). The enhancement of the current may be due to a supply of H^+ from the dissociation of the carboxylic acid adsorbed on the latex. The reduction peak potential was shifted by 0.15 V in the negative direction from that at the Pt electrode. The negative shift may be ascribed to the potential shift in the Nernst equilibrium owing to accumulation of H or H_2 on the electrode. The cathodic peak currents at -0.5 V were approximately proportional to $v^{1/2}$ for a thin layer. They varied to the adsorption-control with an increase in the thickness.

The cathodic peak currents at -0.5 V increased linearly with amounts of the immobilized latex, implying accumulation of H^+ near the electrode, as is shown in Fig. 4(b). Here, the thickness was calculated from the weight of the dried latex and density of the film. The slope, being the current -0.68 μA per particle layer, can be regarded as the adsorption current caused by the one particle layer. If the peak current is assumed to be expressed by $I_p = F^2\Gamma AvRT/4$, the value of the adsorbed amount, Γ, is calculated to be 0.4×10^{-11} mol mm^{-2}, where A is the area of the electrode. In contrast, the adsorbed amount calculated from the number of -COOH per particle by the conductometric titration is 1.3×10^{-11} mol mm^{-2} under the assumption of the closest packed adsorption of the particles. The latter is larger by three times than the former. Since electrode reduction of H^+ can dissociate -COOH partially, the number by the conductometric titration should be larger than the electrochemically reacting number of -COOH.

The oxidation current of FcTMA, in contrast, did not vary appreciably with the amount of the latex, as is shown in Fig. 4(a). FcTMA, possessing one positive charge, has not been taken up to the latex film in salt-rich solutions because of a loss of electrostatic attraction between (latex)-COO^- and FcTMA by salt [25]. Therefore, FcTMA is not accumulated to the electrode, and thus exhibited the thickness-independence.

3.3. Voltammetric features of PAAPS latex at high pH

The conventional technique of fabricating polymer-coated electrode is to spread a polymer solution on an electrode rather than a polymer suspension. We attempted to cast a given amount of tetrahydrofuran(THF)-dissolved PAAPS solution on the platinum electrode and dried the electrode sufficiently, called the THF-PAAPS-coated electrode. The voltammogram at this electrode in the solution of 0.2 mM FcTMA + 0.14 M KCl at pH 5.82 showed the redox wave of FcTMA, as is shown in the solid curve of Figure 5. Since the current values were almost the same as those at the H_2O-PAAPS-coated electrode (-.-) and the bare Pt electrode (...), the THF-PAAPS-coating film is permeable for FcTMA or takes patched form on the electrode. On the other hand, it had no response of the reduction of H^+ at all (see no current at -0.5 V), as contrasted with the wave at the H_2O-PAAPS-coated electrode. When a water droplet was mounted on the THF-PAAPS-coated electrode in air, the contact angle was 80^o. In contrast, the H_2O-PAAPS-coated electrode showed the contact angle 30^o (flatter). The THF-PAAPS-film is more hydrophobic than the H_2O-PAAPS-film. Therefore, the dissociation should be suppressed in the THF-PAAPS-film, and no reduction current of H^+ was observed. The THF-PAAPS-film hindered dissociation, whereas H_2O-PAAPS-film could keep hydrophilicity for the dissociation. This is an advantage of fabrication of films by means of latex techniques.

When pH in the solution was over 5.5 without using buffer solution, dependence of the reduction currents of H^+ on the film thickness and scan rates was different from that for pH lower than 4.5. The current was independent of the film thickness, as is shown in curve (c) of Fig. 4. Only the interfacial domain between the electrode and the film can supply hydrogen ion. In accord with this surface process, the peak currents were proportional to the scan rates for $v < 0.5$ V s^{-1}, as is shown in Fig. 5 at some pH values of the solution. Those at high scan rates deviated lower values from each proportional line. The deviation may be ascribed to participation of diffusion and/or the dissociation kinetics. Since the thickness of the diffusion layer at 1 V s^{-1} is ca 10 μm, diffusion

within the film in one-particle layer thickness (0.26 μm) mush not give rise to the delay of the current. The dissociation kinetics is predicted to be responsible for the deviation. We shall derive equations for peak currents as a function of scan rates and dissociation rate constants when carboxyl acid in a very thin film is dissociated by the electroreduction of H^+.

4. Theory of voltammetric CE reactions in thin films

Analysis of CE reactions of weak acids has been a classical subject in polarography [40] and at the RDE [41,42]. The theory EC reactions in voltammetry has been developed to cyclic voltammetry [43]. These theoretical investigations are modeled on diffusion or convective diffusion complicated by the CE reaction. Theoretical work on voltammetric CE reactions for the surface process has not been reported yet, to our knowledge, and thus we shall describe it here.

We consider the chemical reaction of **2** (HA) $\leftrightarrow$ **1** (H^+) + **3** (A^-), in which species **2** and **3** are electrochemically inactive, and species **1** is reduced at an electrode according to the Nernst equilibrium. The reaction occurs in a thin film with a thickness w, into which **1** and the supporting electrolytes can be penetrated or released without blocking by the film. Species **2** and **3** are confined in the film. Before the electrode reaction occurs, the chemical equilibrium holds, keeping the initial concentrations, $K=c_1^* c_3^* / c_2^*$, where K is the equilibrium constant and c_n is the concentration of species n in the equilibrium. We define the pseudo-equilibrium constant

$$K_p = c_1^* / c_2^* = K / c_3^* \qquad (2)$$

of the reaction

2 (HA) $\leftrightarrow$ **1** (H^+) (3)

When the concentration of species **1**, c_1, decreases due to the reduction at the electrode, **1** is supplied with the dissociation reaction at the reaction rate, $kc_2 - k'c_1$, where k and k' are the dissociation and the association rate constants, respectively. It is assumed that

the film is so thin that the concentration distribution caused by the electrochemical reduction becomes rapidly uniform in the film. Consequently, the concentrations can be represented as the densities of adsorbed amounts, Γ_1 and Γ_2 instead of c_1 and c_2. The rate of Γ_2 obeys simply the reaction kinetics of reaction (3), i.e.,

$$d\Gamma_2/dt = - k\Gamma_2 + k'\Gamma_1 \qquad (4)$$

In contrast, **1** is supplied with the dissociation but is consumed by the electrochemical reduction. Therefore the rate of Γ_1 is given by

$$d\Gamma_1/dt = k\Gamma_2 - k'\Gamma_1 + j/F \qquad (5)$$

where j is the current density by the reduction $H^+ + e^- \rightarrow H$, taking a negative value. Γ_1 is controlled by an electrode potential through the Nernst equation of this reduction. Unfortunately, neither concentration of H nor H_2 is known, and hence an accurate Nernst equation cannot be formulated. An approximated Nernst equation may be helpful only for discussing dependence of peak currents on scan rates rather than the peak potential. We assume that Γ_1 is given by

$$\Gamma_1 = \Gamma_1^* / (1 + e^{-\zeta}) \qquad (6)$$

where Γ_1^* is the initial surface density of H^+ in the film, i.e., equal to $c_1^* w$. Here ζ is the dimensionless potential scanned in the negative direction at the scan rate v

$$\zeta = (E - E^o)F/RT = (- vt + E_{nt})F/RT$$

where E_{nt} is the initial potential for the scan. According to the equilibrium conditions, k, k' and K_p are related to

$$K_p = \Gamma_1^*/ \Gamma_2^* = k / k' \qquad (7)$$

Our goal is to derive an expression for j/F as a function of ζ. Inserting Eq.(6) into Eq.(5) and carrying out the differentiation, we obtain

$$- j/F = k\Gamma_2 - k'\Gamma_1^* / (1 + e^{-\zeta}) + (vF\Gamma_1^*/4RT)\,\mathrm{sech}^2(\zeta/2) \qquad (8)$$

Inserting Eq.(6) into Eq.(4) and solving the differential equation, we have an explicit form for Γ_2

$$\Gamma_2 = \Gamma_2^* e^{-kt} + k'\Gamma_1^* \int_0^t e^{-k(t-u)} \left[1 + \exp\left((F/RT)(vu - E_{nt})\right)\right]^{-1} du$$

It can be rewritten as

$$\Gamma_2 / \Gamma_2^* = \exp\left(\lambda(\zeta - \zeta_{\mathrm{nt}})\right) - \lambda \int_{\zeta_{\mathrm{nt}}}^{\zeta} \mathrm{e}^{\lambda(\zeta - \zeta')} \left(1 + \mathrm{e}^{-\zeta'}\right)^{-1} \mathrm{d}\zeta' \qquad (9)$$

where

$$\lambda = kRT / Fv \qquad (10)$$

$$\zeta_{\mathrm{nt}} = E_{\mathrm{nt}} F / RT$$

Eliminating Γ_2 from Eq.(8) and (9) yield

$$\frac{-j}{kF\Gamma_2^*} = \exp\left(\lambda(\zeta - \zeta_{\mathrm{nt}})\right) - \lambda \int_{\zeta_{\mathrm{nt}}}^{\zeta} \frac{\mathrm{e}^{\lambda(\zeta - \zeta')}}{1 + \mathrm{e}^{-\zeta'}} \mathrm{d}\zeta' - \frac{1}{1 + \mathrm{e}^{-\zeta}} + \frac{K_{\mathrm{p}}}{4\lambda} \mathrm{sech}^2(\zeta / 2) \qquad (11)$$

The first two terms in Eq.(11) are ascribed to the dissociation rate, while the third term is attributed to the association (backward) rate. The forth term represents the reduction of the initially confirmed species **1** because of the equality, $k\Gamma_2^* K_{\mathrm{p}}/\lambda = \Gamma_1^* Fv/RT$.

Figure 7 shows variations of dimensionless voltammograms calculated numerically from Eq.(11) at several values of λ. A bell-shape of the voltammograms is caused by the whole consumption of both **1** and **2** in the film. Although it resembles the simplest surface wave expressed by $\mathrm{sech}^2(\zeta/2)$, the voltammograms are combinations of the exponential, sigmoidal and bell-shaped variations. A peak appears at $\zeta = 0$ or at the potential very close to E^{o}, regardless of K_{p} and λ.

By setting $\zeta = 0$ and $\zeta_{\mathrm{nt}} \to \infty$ in Eq.(11), the dimensionless peak currents, j_{p}, is given by

$$\frac{-j_{\mathrm{p}}}{kF\Gamma_2^*} = \lambda \int_0^{\infty} \frac{\mathrm{e}^{-\lambda\zeta'}}{1 + \mathrm{e}^{-\zeta'}} \mathrm{d}\zeta' - \frac{1}{2} + \frac{K_{\mathrm{p}}}{4\lambda} = \frac{\lambda}{2} \left\{ \psi\left(\frac{\lambda + 1}{2}\right) - \psi\left(\frac{\lambda}{2}\right) \right\} - \frac{1}{2} + \frac{K_{\mathrm{p}}}{4\lambda} \qquad (12)$$

where the definite integral was expressed by the combination of the Psi functions, $\psi(z) = \Gamma'(z)/\Gamma(z)$ [44]. The bracket for the difference in the psi functions has the following expansions:

$\psi((\lambda+1)/2) - \psi(\lambda/2) = 1/\lambda + 1/2\lambda^2 - 1/4\lambda^4 + \ldots$ for large λ

$\psi((\lambda+1)/2) - \psi(\lambda/2) = 2/\lambda - 2 \ln 2 + ...$ for small λ

Then Eq.(12) can be rewritten as

$$-j_p/F \approx (\Gamma_1^* + \Gamma_2^*)Fv/4RT - (\Gamma_2^*/8k^2)(Fv/RT)^3 \quad \text{for large } \lambda \qquad (13)$$

$$-j_p/F \approx \Gamma_1^* Fv/4RT + k\Gamma_2^*/2 \quad \text{for small } \lambda \qquad (14)$$

The first term of Eq.(13) indicates that the current should be supplied from all the amounts of both **1** and **2** for large values of k and at slow scan rates. This corresponds to the maximum value of the peak currents in the model reaction. With an increase in the scan rates, the dissociation rate suppresses the current by the ratio, λ^{-2} (= $(Fv/RTk)^2$). In contrast, the first term in Eq.(14) represents the peak current only for initially existing **1** in the film. The second term means the supply of **1** from the dissociation.

Dependence of the peak current on the scan rates can be represented by the plotting $-j_p/kF\Gamma_2^*$ against $1/\lambda$. Figure 8 shows the dependence for several values of K_p, where the psi functions were evaluated in the way as described in Appendix. The curves have each tangent line at $\lambda^{-1} = 0$ (or $v = 0$), of which functional form is expressed by

$$-(j_p)_{prp}/kF\Gamma_2^* = (1 + K_p)/4\lambda \qquad (15)$$

according to Eq.(13). The peak current should be proportional to the scan rate at lower scan rates. With an increase in v, the current deviates lower from the proportional line. This variation is close to the experimental results in Fig. 6.

We modify Eq.(13) to the form by which the rate constant can be estimated from the peak currents. Dividing Eq.(12) by Eq.(15), and collecting terms including λ on the right hand side, we have

$$[j_p/(j_p)_{prp}](1 + K_p) - K_p = 2\lambda[\lambda\psi((\lambda+1)/2) - \lambda\psi(\lambda/2) - 1] \qquad (16)$$

Values of $[j_p/(j_p)_{prp}](1 + K_p) - K_p$ are plotted against λ in Fig. 9. By taking the current ratio, we can eliminate ambiguity by the amount of the film. Values on the left-hand side are known at some scan rates and a given pH. The working curve (Fig. 9) can provide values of λ from experimental values of j_p, $(j_p)_{prp}$ and K_p. Thus evaluated λ may determine k through Eq.(10).

5. Evaluation of dissociation rate constant

The variations in Fig. 6 have demonstrated the proportionality of the peak current to v for $v < 0.7$ V s^{-1} at any pH value, as is predicted from the theoretical variation in Fig. 8. We drew such proportional lines in Fig. 6 that points $v < 0.7$ V s^{-1} fell on. We evaluated the ratio, $I_p/(I_p)_{prp}$, at each v and pH from the data in Fig. 6. W also obtained values of K_p from some values of pH, pK_a = 5.3 ($K = 10^{-5.3}$) and $c_{HA}^* + c_A^* = 2.7$ M. According to Eq.(1), for example of pH = 6.02, we have $c_A^*/c_{HA}^* = K/c_H^* = 10^{-5.3+6.02}$, and thus $c_A^* = 2.26$ M, $c_{HA}^* = 0.43$ M and $K_p = c_H^*/c_{HA}^* = 2.2\times10^{-6}$. The condition of the pseudo reaction, $c_A^* > c_{HA}^*$ can be approximately satisfied. Since values of K_p are much smaller than unity, the left-hand side of Eq.(16) is numerically the same as $I_p/(I_p)_{prp}$. We read values of λ corresponding to $I_p/(I_p)_{prp}$ from the working curve in Fig. 9, and plotted the inverse values against v for each value of pH in Fig. 10. The values of λ^{-1} were proportional to v, in accord with Eq. (10). The slope, F/RTk, allowed us to evaluate k at some values of pH. Values of k, as listed in Table 1, showed slight dependence on pH. We have employed Eq.(2) for the equilibrium relation although the actual equilibrium is complicated with the electrostatic interaction to be expressed by curve (a) in Fig. 2. By tracing a horizontal line at pH 6 in Fig. 2, we find that a value of x or c_H^* on curve (a) of the PAAPS suspension is smaller than that on curve (b) of the dissolved PAAPS. Therefore c_H^* was underestimated in the analytical expression with an increase in pH, and hence provided lower values of k.

It is interesting to compare the dissociation rate constant of the adsorbed latex with that of acrylic acid dissolved in solution. We obtained voltammograms of the solution of 65 mM acrylic acid at pH 5.06, as is shown as curve (c) in Fig. 3. Since the reduction peak at -0.6 V was much larger than the value predicted from diffusion of H^+ in the solution bulk, it should be supplied by the dissociation of acrylic acid. From the pH-titration, the value of pK_a of acrylic acid was 4.25. This value and the total concentration, $c_{HA}^* + c_A^* = 65$ mM, led us to have $c_A^* = 56$, mM $c_{HA}^* = 9$ mM and K_p =

1.0×10^{-3} at pH 5.06. Thus the condition of the pseudo-reactions can be satisfied. The voltammetric peak current of the first order-pseudo CE reaction has been expressed by [43]

$$I_{d,p} / I_p = 1.02 + 0.471\ K_p^{-1} \lambda^{-1/2} \quad (17)$$

where $I_{d,p}$ is the diffusion-controlled peak current. It can be rewritten as

$$1/ I_p = 1.02/ I_{d,p} + 1 / I_k \quad (18)$$

where

$$I_k = 0.947AFc_{HA}^{*} (1 + K_p)^{3/2} K_p^{1/2} k^{1/2} D_H^{1/2} \quad (19)$$

Since I_k has no term of v and $I_{d,p}$ is proportional to $v^{1/2}$, Eq.(18) indicates that $1/I_p$ should show a linear relationship with $v^{-1/2}$. Figure 11 shows variation of $1/I_p$ with $v^{-1/2}$, revealing a line. The value of the slope agreed with the theoretical value, $1.02/[0.446AF(c_{HA}^{*}+ c_H^{*})(D_{HA}F/RT)^{1/2}]$, for $D_{HA} = 0.68\times10^{-5}$ cm^2 s^{-1}. The inverse of the intercept is given by Eq. (19). From known values of c_{HA}^{*}, K_p and $D_H^{1/2}$, we obtain k $=1.4\times10^3$ s^{-1}. Dissociation rate constants of other weak acids range from 10^3 to 10^5 s^{-1} [45]. This is larger by one order magnitude than the value at the H_2O-PAAPS-coated electrode. The dissociation at the H_2O-PAAPS-coated electrode occurs in such highly concentrated carboxylic acid in PAAPS that the electric interaction among -COO$^-$ hinders the dissociation. Furthermore, it occurs at the solid surface rather than a homogeneous reaction in solution. Consequently the rate constant should be depressed.

6. Conclusion

The PAAPS latex was a copolymer of PAA and PS, the molar ratio of which was $c_a/c_s = 0.34$, determined by UV. This ratio was five times larger than the loaded ratio in the synthesis. The amount of carboxyl acid to be dissociated was 3 %, implying that the dissociation should be restricted to the surface domain of 1.5 nm. The limited domain of the dissociation may be ascribed to hydrophobicity of the phenylethyl group of PS. Despite the small ratio of dissociation, the average concentration of effective carboxyl

group was 0.7 M (= 2.7 M ×0.34)/(0.34+1)), which can work as a proton source.

The value of pK_a of the PAAPS latex was larger than that of acrylic acid. The larger value may be caused by the electrostatic interaction among deprotonated carboxyl groups as well as the hydrophobicity in the latex. The participation in the electrostatic interaction has been revealed to the larger slope in the plot of pH against log[x/(1-x)] than in the ideal plot. In other word, the dissociation is more depressed with an increase in pH.

Voltammograms in the PAAPS suspension at the Pt electrode showed the cathodic current of H^+, the source of which is not only the bulk H^+ but also the dissociation in the adsorbed latex. The reduction current of H^+ at low pH was proportional to the film thickness without blocking of mass transport because of a supply of H^+ by the dissociation in equilibrium. That at pH over 5.5 was, however, independent of the film thickness. With an increase in the scan rate, the current varied from the v-proportionality to the lower deviation. This variation demonstrates a participation in the dissociation kinetics.

Expressions for the voltammograms of the adsorbed carboxyl moiety with the EC mechanism were derived under the condition of the first order-pseudo reaction without mass transport. The kinetically controlled peak current was related with the kinetic parameter. The dependence of the theoretical peak current on v was similar to the experimental results. This dependence allowed us to evaluate the dissociation rate constant. The technique of just taking the current ratio eliminates experimental artifacts of amounts of the adsorbed species and their non-uniformity. The value was larger by one order magnitude than that of acrylic acid in the homogeneous reaction, probably because of the electrostatic interaction of $-COO^-$, hydrophobicity and solid phase reaction.

Advantages of making latex-originated PAA film on an electrode are (i) such high permeability of ions and solvent into the film that the current is controlled by diffusion, (ii) control of film thickness by addition of given amounts of the suspension, and (iii)

retaining ion-exchange properties similar to those of acrylic acid. The ionic and voltammetric behavior of the PAAPS suspension is closer to that of dissolved poly(acrylic acid) than the conventional poly(acryl acid) film. However, it is necessary to take into consideration the limitation of reactive zone due to hydrophobicity.

Appendix

The psi function has an analytical form only when its argument is a rational number, m/n, for integers m and n with $m < n$. The expression is given by [44]

$$\psi(m/n) = -\gamma - \ln n - \frac{\pi}{2}\cot\frac{m}{n}\pi + \sum_{k=1}^{n-1}\cos\frac{2km\pi}{n}\ln\left(2\sin\frac{k\pi}{n}\right) \qquad \text{(A1)}$$

where γ is Euler's constant, 0.57721. Values of $\psi(m/n)$ for $n = 2500$ at m from 1 to 2499 were computed to make a table for ψ. Values of $\psi(x)$ for any value of $0 < x < 1$ were determined by interpolation by use of the table. Those for $x > 1$ were obtained by iterative use of the recurrence formulas,

$$\psi(x + 1) = \psi(x) + 1/x \qquad \text{(A2)}$$

References

[1] K. Anbalagan, P. Natarajan, J. Polym. Sci. A 29 (1991) 1739.

[2] A. P. Taylor, J. A. Crayston, T. J. Dines, Analyst 123 (1998) 1913.

[3] M. Plavsic, B. Cosovic, Colloids Surf. A 151 (1999) 189.

[4] A. Goekceoeren, C. Erbil, E. Sezer, J. Appl. Electrochem. 37 (2007) 941.

[5] C. O. Dasenbrock, T. H. Ridway, C. J. Seliskar, W. R. Heineman, Electrochim. Acta 43 (1998) 3497.

[6] Y. Kashiwagi, C. Kikuchi, J. Anzai, J. Electroanal. Chem. 518 (2002) 51.

[7] M. Tagliazucchi, F. J. Williams, E. J. Calvo, J. Phys. Chem. B 111 (2007) 8105.

[8] R. Jiang, F. C. Anson, J. Phys. Chem. 96 (1992) 10565.

[9] O. Hatozaki, F. C. Anson, J. Phys. Chem. 100 (1996) 8448.

[10] W. Hyk, M. Ciszkowska, J. Phys. Chem. B. 103 (1999) 6466.

[11] M. Masiak, W. Hyk, Z. Stojek, M. Ciszkowska, J. Phys. Chem. B 111 (2007) 11194.

[12] V. P.-Yissar, E. Katz, O. Lioubashevski, I. Willner, Langmuir 17 (2001) 1110.

[13] J. Zhou, X. Lu, J. Hu, J. Li, Chem. A Eur. J. 13 (2007) 2847.

[14] A. Liu, T. Watanabe, I. Honma, J. Wang, H. Zhou, Biosens. Bioelectron. 22 (2006) 694.

[15] S. Pinijsuwan, P. Rijiravanich, M. Somasundrum, W. Surareungchai, Anal. Chem. 80 (2008) 6779.

[16] L. Sheeney-Haj-Ichia, Z. Cheglakov, I. Willner, J. Phys. Chem. B, 108 (2004) 11.

[17] M. Z. Markarian, M. E. Harakeh, L. I. Halaoui, J. Phys. Chem. B 109 (2005) 11616.

[18] Y. Xian, F. Liu, L. Feng, F. Wu, L. Wang, L. Jin, Electrochem. Commun. 9 (2007) 773.

[19] T.F. Otero, M.J. Gonzfilez-Tejera, J. Electroanal. Chem. 429 (1997) 19.

[20] O. A. Raitman, E. Katz, A. F. Buckmann, I. Willner, J. Am. Chem. Soc. 124 (2002) 6487.

[21] K. Aoki, T. Kakiuchi, J. Electroanal. Chem. 478 (1999) 101.

[22] V. Kane, P. Mulvaney, Langmuir 14 (1998) 3303.

[23] K. Hu, A.J. Bard, Langmuir 13 (1997) 5114.

[24] T. Fushimi, A. Oda, H. Ohkita, S. Ito, Thin Solid Films 484 (2005) 318.

[25] K. Aoki, T. Li, J. Chen, T. Nishiumi, J. Electroanal. Chem. 613 (2008) 1.

[26] Y. Gao, J. Chen, J. Electroanal. Chem. 578 (2005) 129.

[27 Y. Gao, J. Chen, J. Electroanal. Chem. 583 (2005) 286.

[28] P. Rijiravanich, K. Aoki, J. Chen, W. Surareungchai, M. Somasundrum, Electroanalysis 16 (2004) 605.

[29] C. Xu, J.Chen, K.Aoki, Electrochem. Commun. 5 (2003) 506.

[30] C. Xu, K. Aoki, Langmuir 20 (2004) 10194.

[31] J. Chen, Z. Zhang, J. Electroanal. Chem. 583 (2005) 116.

[32] L. Han, J. Chen, K. Aoki, J. Electroanal. Chem. 602 (2007) 123.

[33] L. Han, J. Chen, I. Ikeda, Chem. Let. 34 (2005) 1512.

[34] K. Aoki, Electrochim. Acta, 51 (2006) 6012.

[35] K. Aoki, T. Lei, Langmuir, 16 (2000) 10069.

[36] K. Aoki, Q. Ke, J. Electroanal. Chem., 587 (2006) 86.

[37] H. Chen, J. Chen, K. Aoki, T. Nishiumi, Electrochim. Acta, 53 (2008) 7100.

[38] G. Bidan, M.-A. Niel, Synth. Met. 85 (1997) 1387.

[39] M. Plavsic, B. Cosovic, S. Rodic, Colloid Polym. Sci. 274 (1996) 548.

[40] J. Heyrovsky, J. Kuta, Principles of Polarography, Academic Press, 1966, New York

[41] W.J. Albery, Electrode Kinetics, Oxford University Press, 1975.

[42] B. G.-Mihelcic, W. Vielstich, Ber. Bunsenges. Phys. Chem.,77 (1973) 476.

[43] R. S. Nicholson, I. Shain, Anal. Chem. 36 (1964) 706.

[44] M. Abramowitz and I. A. Stegun, Handbook of Mathematical Functions, National Bureau of Standards Applied Mathematics Series - 55, Washington,1972, p. 258-259.

[45] S. Daniele, I. Lavagnini, M. A. Baldo, F. Magno, Anal. Chem. 70 (1998) 285.

Figure Captions

Figure 1. pH-titration curve of 20 cm^3, 12.8 mg dm^{-3} PAAPS suspension when the suspension including 0.8 M NaCl was titrated with 0.012 M NaOH, where V_{NaOH} is the titrated volume. The suspension was initially acidified with 0.1 M HCl, and was centrifuged with ultrapure water three times.

Figure 2. Variations of pH with logarithmic concentration ratios for (a) PAAPS suspension, (b) 0.09 g PAA dissolved in 10 cm^3 THF + 10 cm^3 H_2O + 3 M KCl 1 cm^3 and (c) carboxylalkanethiol self-assembled monolayer, where x = $[NaCl]_{titrated}$ / $[NaCl]_{stoickometric\ point}$. Slopes of the lines for (a) and (c) are 2.0, whereas the slope for (b) is 1.0.

Figure 3. Voltammograms of 0.23mM HCl + 0.20 mM FcTMA + 0.15M KCl at (a) the bare electrode and (b) the H_2O-PAAPS-coated electrode for v = 0.1 V s^{-1}. The voltammogram (c) is for 65 mM acrylic acid + 0.15 M KCl at v = 0.1 V s^{-1}, where the current values were reduced to five times from the y-scale.

Figure 4. Film thickness-dependence of (a) the anodic peak currents of FcTMA and (b) the cathodic peak currents of H^+ in 2 mM HCl + 0.2 mM FcTMA + 0.15 M KCl solution at v = 0.1 V s^{-1}, where N is the number of particle layers, e.g., N = 1 corresponding to 0.265 μm. Plot (c) is for the cathodic peak currents of H^+ at the H_2O-PAAPS-coated electrode in the solution of 0.2 mM HCl + 0.2 mM FcTMA + 0.15 M KCl at v = 0.1 V s^{-1}.

Figure 5. Voltammograms in 0.2 mM FcTMA + 0.15 M KCl solution for pH 5.82 at (solid) THF-PAAPS-coated electrode, (-.-) H_2O-PAAPS-coated electrode and (...) bare Pt electrode.

Figure 6. Scan rate dependence of the cathodic peak currents of H^+ in 0.2 mM FcTMA + 0.15 M KCl solution at the H_2O-PAAPS-coated electrode when pH was adjusted to (a) 5.82, (b) 6.02, (c) 6.20 and (d) 6.40 by addition of HCl.

Figure 7. Dimensionless linear sweep voltammograms calculated from Eq.(11) for K_p = 100 at λ (=kRT/vF) = (a) 1, (b) 2, (c) 4, (d) 8 and (e) 16.

Figure 8. Variations of dimensionless peak currents with the scan rates for K_p = (a) 5, (b) 2, (c) 1, and (d) 0.2, computed from Eq.(12). The dotted line is a tangent line at $\lambda^{-1} = 0$ for curve (c).

Figure 9. Variation of $[j_p / (j_p)_{prp}] (1 + K_p) - K_p$ with λ, given by Eq.(16).

Figure 10. Plots of λ^{-1} determined from $I_p/(I_p)_{prp}$ in Figure 5 against v for (a) 5.82, (b) 6.02, (c) 6.20 and (d) 6.40.

Figure 11. Plot of I_p^{-1} against $v^{-1/2}$ for the cathodic wave at -0.55 V on the solution of 65 mM acrylic acid + 0.15 KCl solution at the Pt electrode.

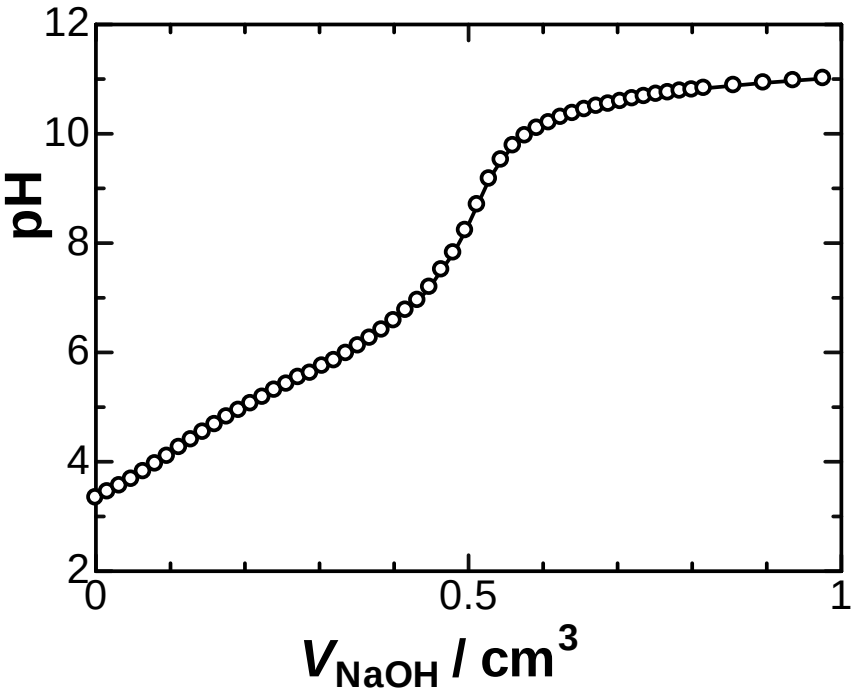

Figure 1

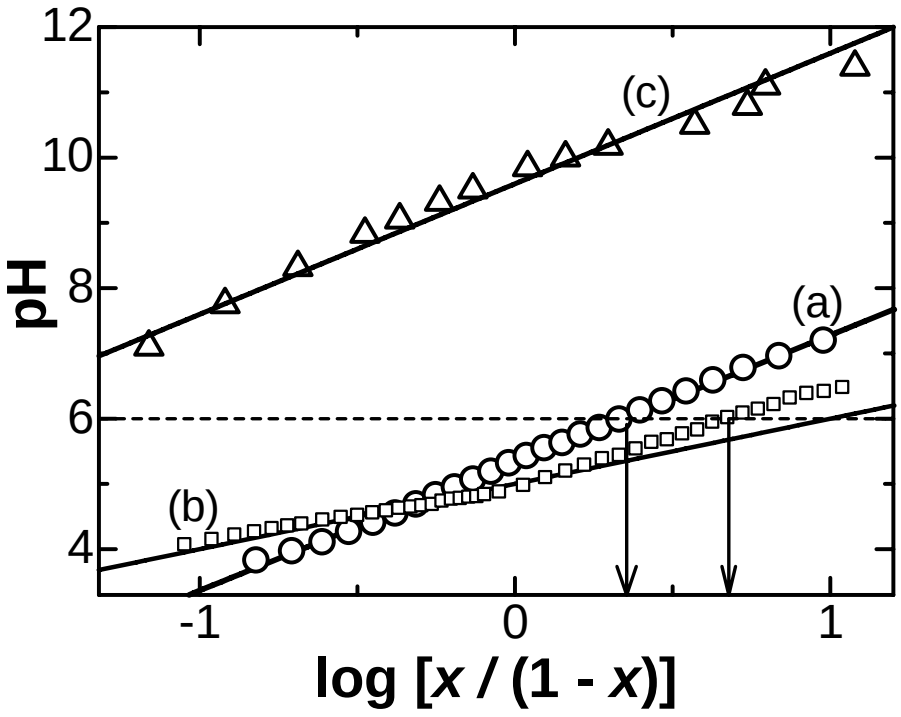

Figure 2

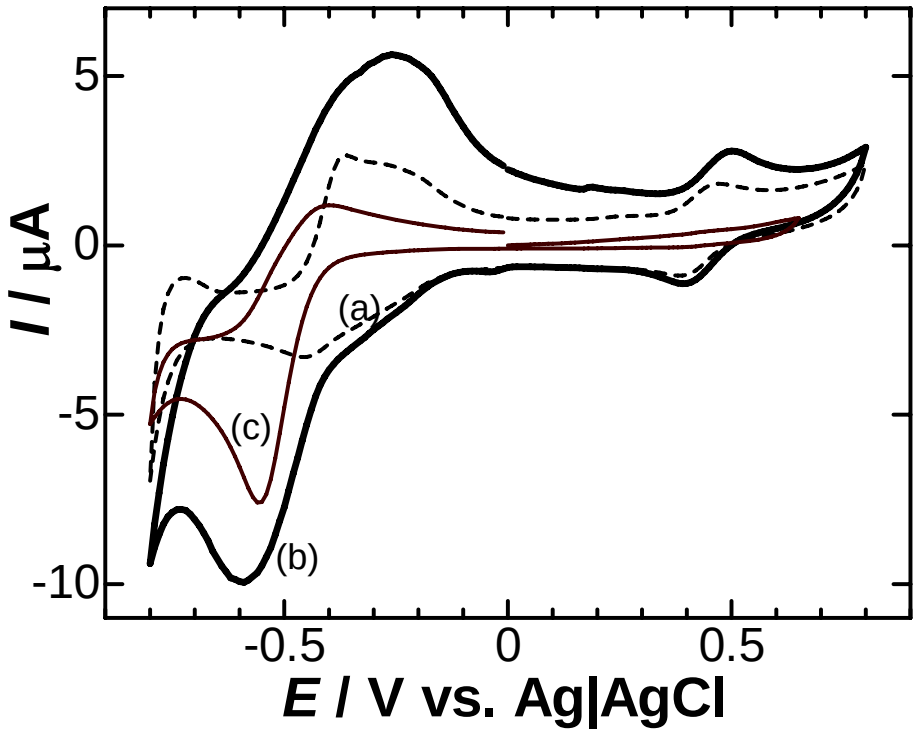

Figure 3

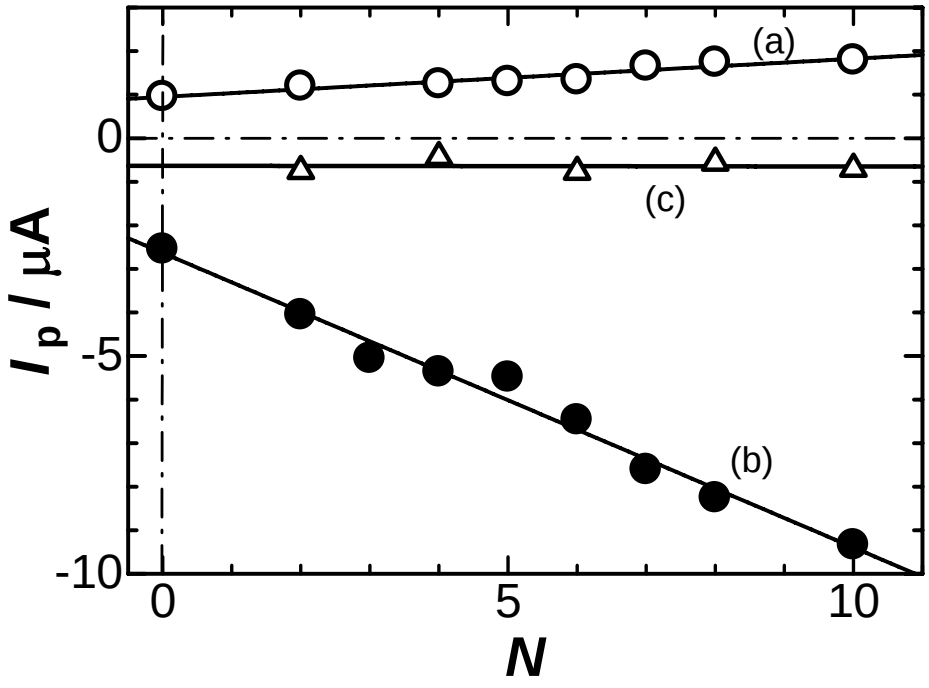

Figure 4

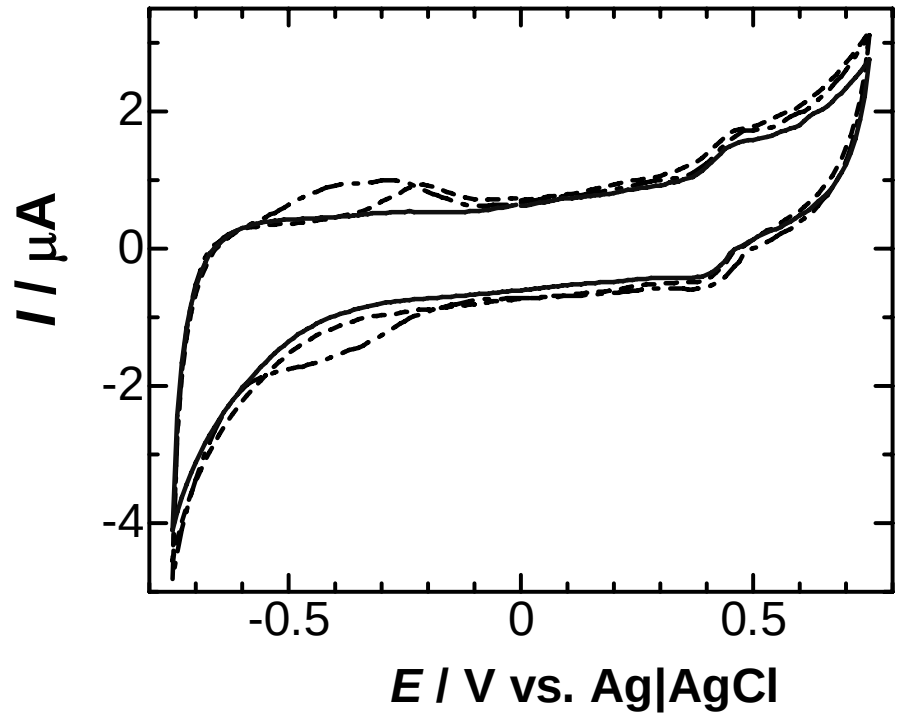

Figure 5

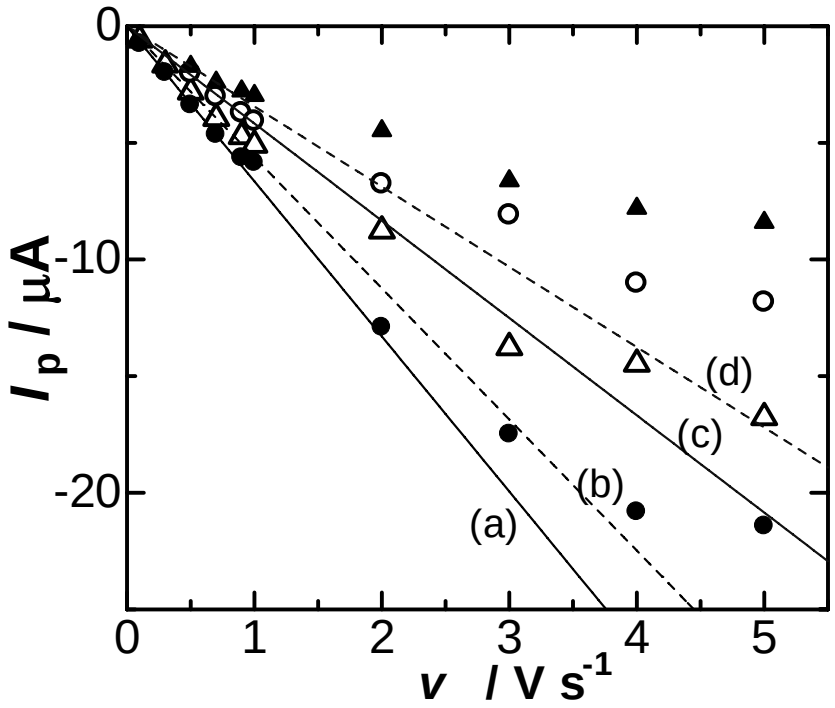

Figure 6

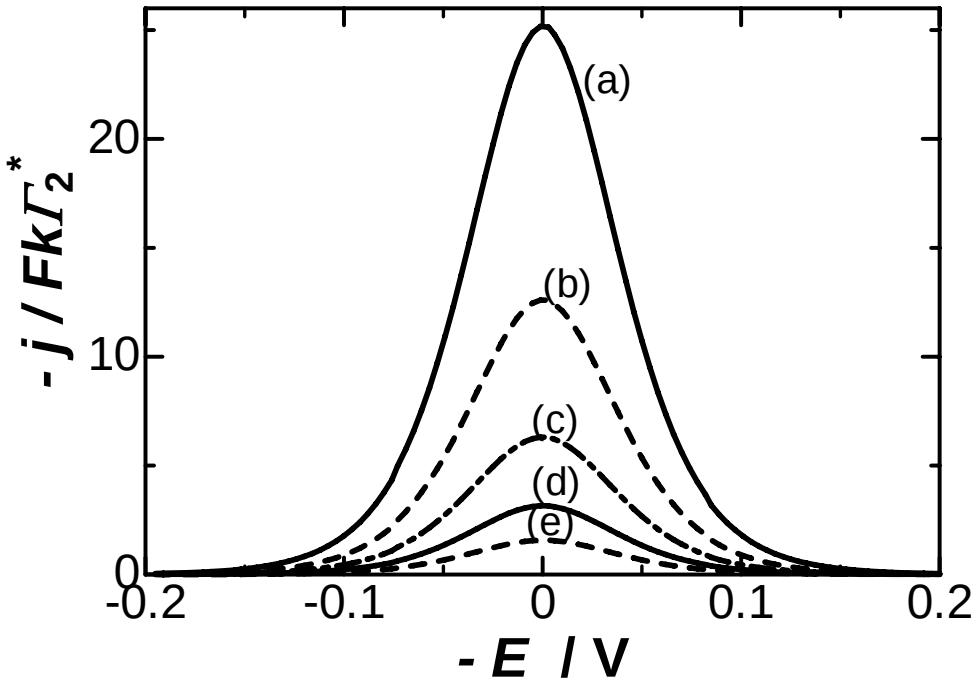

Figure 7

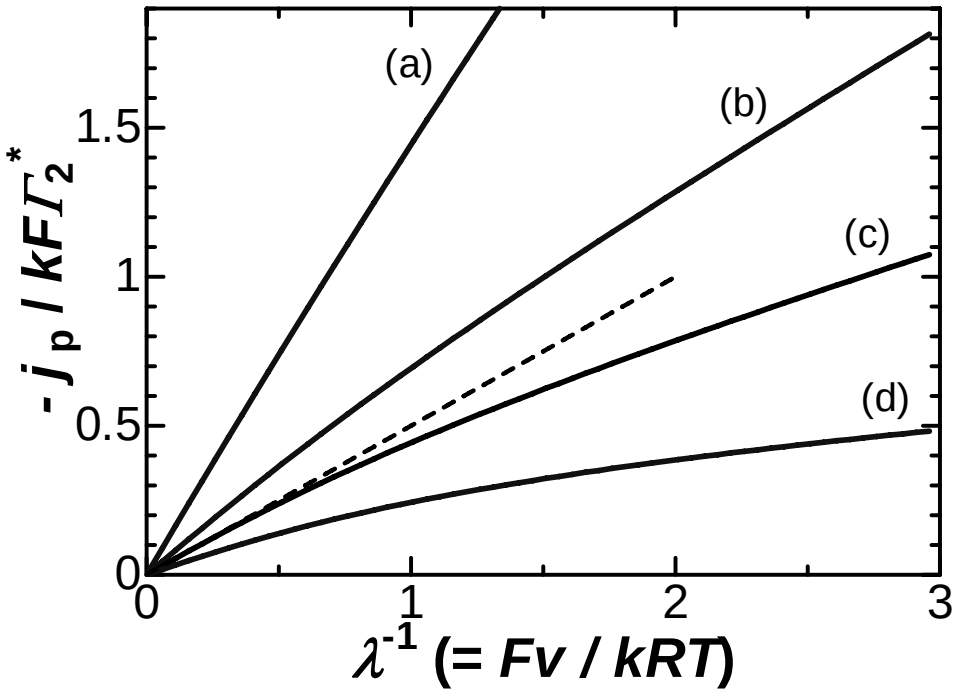

Figure 8

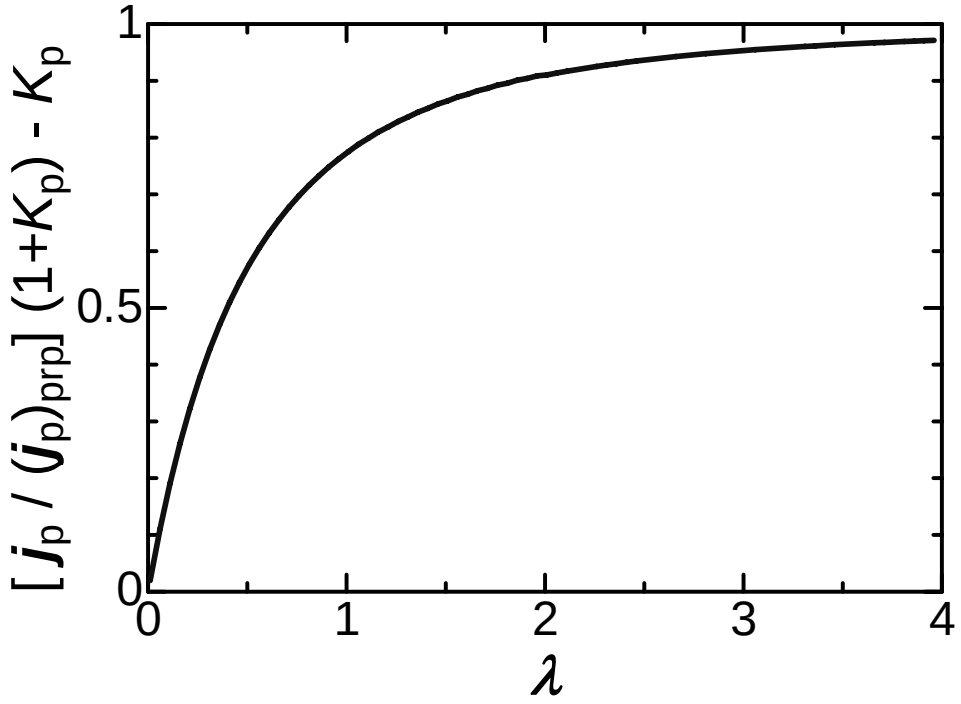

Figure 9

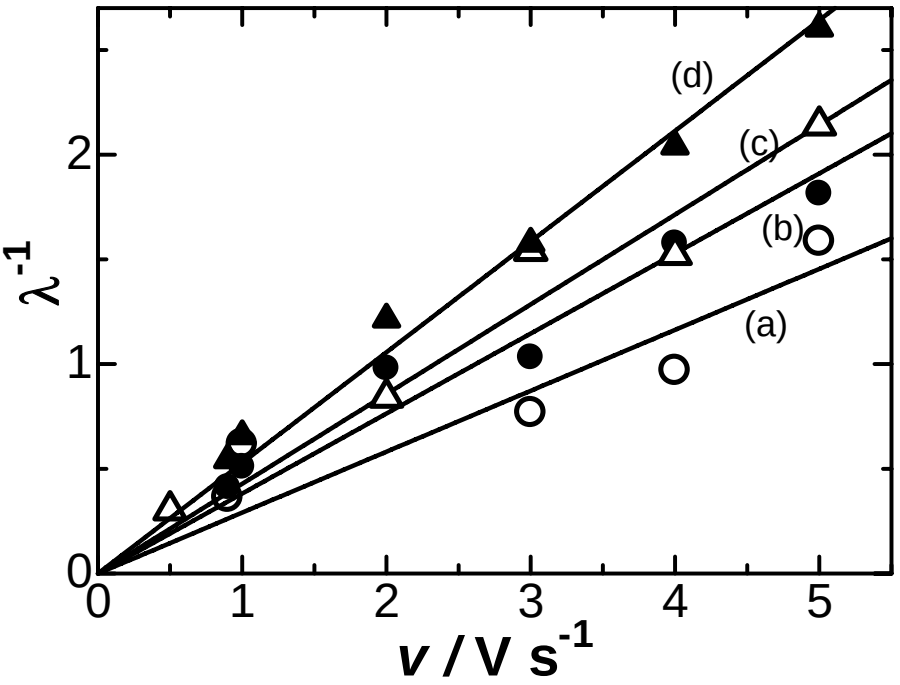

Figure 10

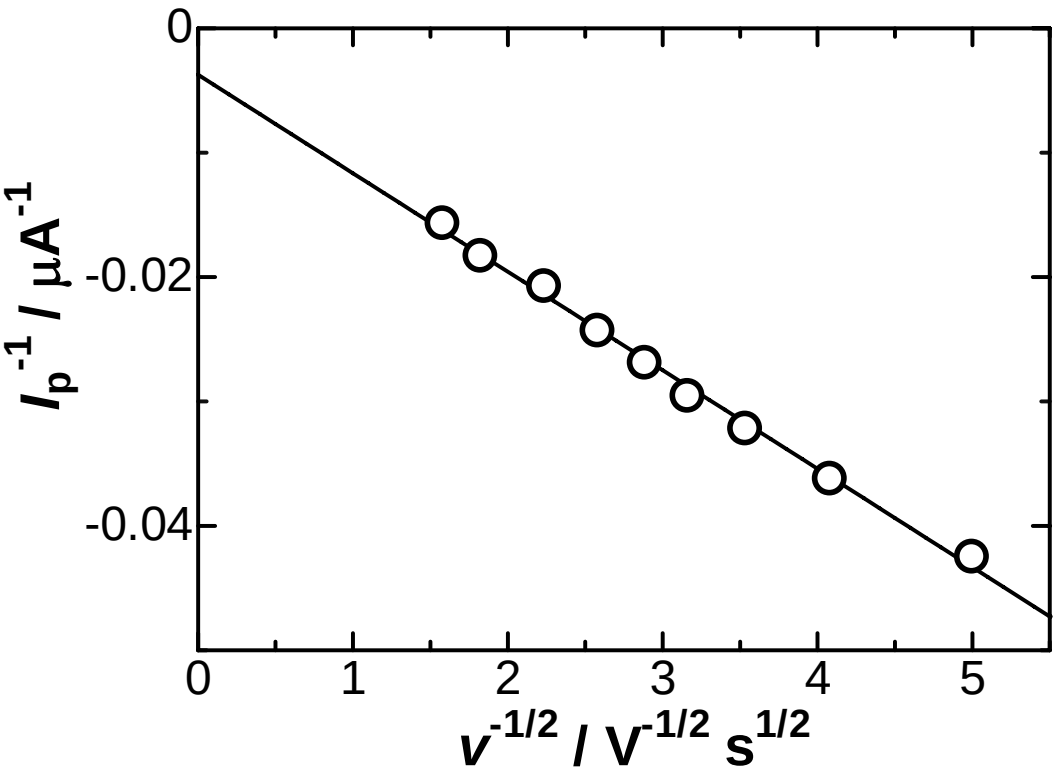

Figure 11

Table 1. Dependence of values of the dissociation rate constants on pH.

pH	$k \times 10^{-2}$ / s
5.82	1.4
6.02	1.0
6.20	0.9
6.40	0.8